https://doi.org/10.22226/2410-3535-2020-4-481-485 PACS: 68.90.+g

A facile synthesis of Cr doped WO_3 nanocomposites and its effect in enhanced current-voltage and impedance characteristics of thin films

V. M. Adimule[†,1], D. Bowmik[2], H. J. Adarsha[3]

[†]adimulevinayak@yahoo.in

[1]Department of Chemistry, Angadi Institute of Technology and Management (AITM), Savagaon Road, Belagavi 5800321, Karnataka, India
[2]High Energy Materials Research Laboratory, Defence Research and Development Organization, Ministry of Defence, Government of India, Sutarwadi, Pune-411021, India
[3]Centre for Research in Medical Devices, National University of Ireland, Gaillimh, Galway- H91TK33, Ireland

In this study we report the enhanced impedance and current-voltage (*I-V*) characteristics of Cr doped WO_3 in different % weight (5, 8, 15 wt.%) ratio, synthesized by co- precipitation method using surfactants. Nanostructures (NS) were characterized by cyclic voltammetry (CV), scanning electron microscopy (SEM), X-ray diffraction (XRD) and UV-Visible (UV-Vis) spectroscopy. The pelletized samples performed *I-V* and impedance measurements. The impedance results reveal that the pelletized samples of highest doped Cr showed remarkable increase in the admittance with respect to the biased voltage. *I-V* characteristics of the highest doped Cr showed enhanced surface conductivity as compared with the observed resistance and applied current. The output power considerably increases for 15 wt.% of Cr doped WO_3 and as the doping percentage of Cr increases surface conductivity, power output, admittance values considerably enhances in the material matrix. This work demonstrated that Cr doped WO_3 has more current sensitivity and selectivity towards *I-V*, impedance, admittance value which considerably varies with the applied bias voltage. Nano particles (NPs) of Cr-WO_3 can be a versatile material for the superconductor, biosensors, sensing of various gases as its greater value of impedance can help in its use in electronic devices stimulus detection of various gases and super capacitor applications.

Keywords: nanostructures, Cr, WO_3, current-voltage characteristics, impedance, admittance.

УДК: 538.9

Простой синтез нанокомпозитов WO_3, легированных хромом, и его влияние на улучшенные вольт-амперные и импедансные характеристики тонких пленок

Адимюль М. В.[†,1], Боумик Д.[2], Адарша Х. Дж.[3]

[1]Департамент химии, Ангудийский институт технологии и менеджмента, Савагаонское ш., Белагави, 5800321, Карнатака, Индия
[2]Лаборатория исследований высокоэнергетических материалов, Организация оборонных исследований и разработок, Министерство обороны, Правительство Индии, Сутарвади, Пюн-411021, Индия
[3]Центр исследований медицинских устройств, Национальный университет Ирландии, Гайлим, Голуэй- H91TK33, Ирландия

В этом исследовании сообщается об улучшенных импедансных и вольт-амперных характеристиках WO_3, легированного Cr в различных весовых процентах (5, 8, 15 мас.%), синтезированных методом соосаждения с использованием поверхностно-активных веществ. Наноструктуры были охарактеризованы с помощью циклической вольтамперометрии, сканирующей электронной микроскопии, рентгеновской дифрактографии и ультрафиолетовой и видимой спектроскопии. Для гранулированных образцов проводили измерения ВАХ и импеданса. Из результатов по импедансу видно, что гранулированные образцы с самым высоким содержанием легированного Cr показывают заметное увеличение проводимости по отношению к напряжению смещения. ВАХ наиболее легированного Cr показали повышенную поверхностную проводимость по сравнению с наблюдаемым

сопротивлением и приложенным током. Выходная мощность значительно увеличивается на WO_3, легированного 15 мас.% Cr, и поскольку процентное содержание легирования Cr увеличивает поверхностную проводимость, выходная мощность, значения проводимости в матрице материала значительно улучшаются. Работа демонстрирует, что WO_3, легированный хромом, имеет большую чувствительность по току и селективность в отношении *I-V*, импеданса, значения проводимости, которое значительно меняется в зависимости от приложенного напряжения смещения. Наночастицы Cr-WO_3 могут быть универсальным материалом для сверхпроводников, биосенсоров, обнаружения различных газов, поскольку их большее значение импеданса может помочь в его использовании в электронных устройствах, стимулирующих обнаружение различных газов и применения суперконденсаторов.

Ключевые слова: наноструктуры, Cr, WO_3, вольтамперные характеристики, импеданс, проводимость.

1. Introduction

In recent years nano science and nanotechnology [1–4] emerged as new materials and many functional nanocomposites (NCs) with modified facilities were incorporated. In recent times materials adopted for device fabrication in nano electronics [5,6] played important role. Growing areas in nano chemistry, functional nano metered sized particles, especially metallic particles show considerable change in the electrical and electronic properties [7–10]. As compared with the bulk scale materials, especially materials of hybrid nanocomposites of organic and inorganic nanostructures find their applications in electrical components and devices [11,12].Thus, these materials are designed and investigated largely. In order that the materials to show enhanced properties for the solar cells [13], sensors [14], optics [15], photodiodes [16], and LEDs [17] etc. nanomaterials synthesized in proper shape and size generally, specific size, shape and uniform distribution of the particle are achieved by varying the synthetic methods [18], different reducing agents, stabilizers etc. In co precipitation method [19, 20] of chemical approach of the synthesis, metal cations and anions are combined and allowed to form clusters and aggregates. Cr NPs have been reported for increased *I-V* [21], photo electro chemical [22], photoluminescence [23], optical [24], sensors [25] and electrical and electronic properties [26]. Dan Meng et al [27] reported the effect of WO_3 nanostructures in selectively sensing nitrogen dioxide gas and their utility in fabrication of new sensing devices. The Cr doped nanostructures reported by Pratibhavaram et al [28] recently and explained the rapid synthetic methods, applications in the photo catalytic activity. Review of the WO_3 nanoparticles, their applications as electrode, sensor selectivity, sensor response and electrochemical energy storage system discussed by Pragati et al [29]. Wenjie Li et al reported the synthesis of WO_3 nano flakes and their electrochemical conversion, electrical resistance, impedance and power dissipation [30] in recent years. Zhengyou Zhu et al reported [31] high selectivity of the Cr doped WO_3 nanostructures and their applications in the detection of 3-hydroxybutanone biomarker in electrochemical system. In the present study wet, economical co precipitation method of synthesis of Cr doped WO_3 NPs, their current-voltage and impedance measurements in pelletized structures, implications in the material properties of Cr doped WO_3. Author envisaged that the effect of Cr doping on WO_3 nanostructure may increase the current gain, voltage gain impedance, admittance and power dissipation factor of the pelletized nanomaterials. Present research gives path way for the developing new and emerging materials for the gas sensors, biosensors, photovoltaic materials, optical and photo luminescent, LED materials.

2. Materials and methods

Material required for the synthesis are procured from Sigma Aldrich, spectrochem, Sd-fine chemicals and used without any purification. Deposition of the Cr doped WO_3 NPs is done using RF spluttering instrument procured from advanced process technology, morphology of the pure WO_3 and Cr-WO_3 NPs investigated by solid supported SEM-EDS Zeiss Ultra 55 instrument with integrated energy and angle back scattered electron detector (EsB). Powdered XRD (X-ray diffractometer) instrument from Rigka Smart Lab with Bragg-Brentano (BB) and parallel beam (PB) optics, with a hypix-3000 high energy resolution 2D multidimensional semiconductor detector having $Cu_{K\acute{a}}$-radiation (l = 0.1542 nm) operating at 50 kV and 40 mA used in determining the shape, size and structures of pure WO_3 and Cr-WO_3 nanoparticles. Optical properties of the pure WO_3 and Cr-WO_3 nanoparticles investigated by UV-Visible absorption spectrum which was recorded using specord 210 plus analytic jena equipped with variable spectral resolution. CV was performed by using CHI company USA (Austin) electrochemical analyzer model D 630. The *I-V* experiments were carried out by using Agilent B 1500 A series instrument (Key Sight Technology) with pulsed source of 5 MHz measurements from 1 KHz to 5 MHz, 10 ns pulsed *I-V* resolution.

3. Experimental

3.1. Synthesis of WO_3 nanoparticles (step 1)

$Na_2WO_4 \cdot 2H_2O$ (1mole) was added with analytical grade 3N solution of HCl under stirring, pH was maintained in between 1–2, a specific amount of triethanol amine was added after 1–2 h of stirring and reaction mixture was heated to 100°C for 2–3 h, precipitate obtained by adding NH_4OH solution was filtered, washed with water, ethanol to remove the surface bound impurities and dried at 100–200°C, calcinated at 800°C to obtain WO_3 NPs. Reactions shown in Fig. 1S (Supplementary Material).

Reactions:

$$Na_2WO_4(s) + 2HCl(l) \rightarrow WO_3(s) + 2NaCl(s) + H_2O(l)$$

$$WO_3(s) \rightarrow WO_2(s) + ½O_2(g)$$

$$WO_2(s) + ½O_2(g) \rightarrow WO_3(s)$$

3.2. Doping Cr to WO_3 Nanostructures (step 2)

Chromium (III) nitrate nona hydrate (5, 10, 15 wt.%) was taken in a round bottom flask added with 3N HCl and mixed with WO_3 NPs obtained from step 1, kept stirring at room temperature overnight. Reaction mixture was heated to 100°C and agitated for 1–2 h, after the ageing for 15 h brown precipitated of Cr doped WO_3 nanostructures was ultrasonicated and filtered, washed with cold water, ethanol, dried at 100°C and calcinated at 750–800°C, grounded to fine powders.

Reactions:

$$Cr(NO_3)_3 \cdot 9H_2O(s) + 3H_2O(l) \rightarrow \rightarrow Cr(OH)_3(s) + 3HNO_3(l) + 9H_2O(l)$$

$$2Cr(OH)_3(s) \rightarrow Cr_2O_3(s) + 3H_2O(g)$$

$$Cr_2O_3(s) + 2WO_2(s) + ½O_2(g) \rightarrow 2Cr\text{-}WO_3(s) + O_2(g)$$

4. Results and discussions

4.1. Cyclic voltammetry

Redox potentials were recorded by using CV as illustrated in Fig. 1 the oxidation potential for the 15 wt.% of Cr doped WO_3 was found to be −0.60 eV with applied voltage varying from 0.1 to 1.6 V and the reduction potential found to be very minimum (+0.08) indicating the complete donor characteristics of the doped chromium due to increased donating ability of the Cr material to the WO_3 with the creation of the band gap of 1.46 eV. Increase in the incorporation of Cr impurity increases the oxidation potentials of the Cr-WO_3 nanostructures.

4.2. Scanning electron microscope (SEM) morphology

SEM images of pure WO_3 (Fig. 2a) and Cr-WO_3 as shown in the Fig. 2. Uniformity and purity of the SEM arrays as represented in picture depicts the pore diameter, wall thickness, interpore distance, and the length of the Cr doped nanostructures (15 wt.%) are ~90, ~85, ~60 and ~75 nm respectively with purity of the Cr-WO_3 (15 wt %) is found to be 97.9%. However, 5 and 8 wt.% of Cr-WO_3 NPs possesses pore diameter, wall thickness, interpore distance, and the length of the Cr ~95, ~100, ~70 and ~85 nm respectively. The transformation of tetragonal structure of WO_3 nanoparticles into nano rod like structures with particle agglomeration can be clearly seen in Fig. 2 b, c, d respectively. Average grain size of the Cr dispersed particle in the inorganic WO_3 nano matrix was found to be ~60 nm and the grain boundary distance is ~90 nm. Chemical compositional analysis and purity of Cr-WO_3 NPs tabulated in Table 1S (Supplementary Material).

4.3. UV-Visible characterization (optical properties)

Different wt.% of Cr doped WO_3 NS recorded for UV-Visible spectrophotometer (Fig. 3). Fig. 3 shows the overlay absorption spectra of the pure WO_3, 5, 8 and 15 wt.% of Cr doped WO_3 nanostructures. Maximum absorptivity was observed for pure WO_3 nanostructure was 295 nm and for 5 wt.% of Cr doped WO_3 nanostructure was 545 nm, 8 wt.% of Cr-WO_3 was 600 to 800 nm and 15 wt.% of Cr-WO_3 UV maxima observed at 800 nm (visible region). Cr impurity

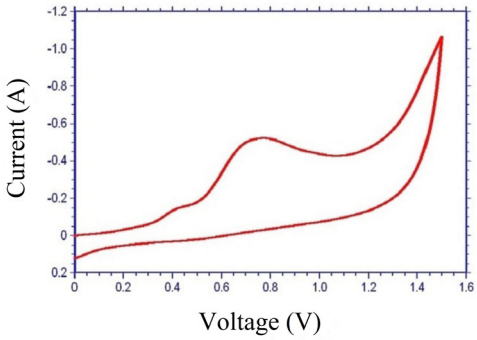

Fig. 1. CV graph of 15 wt.% of Cr doped WO_3 nanostructures.

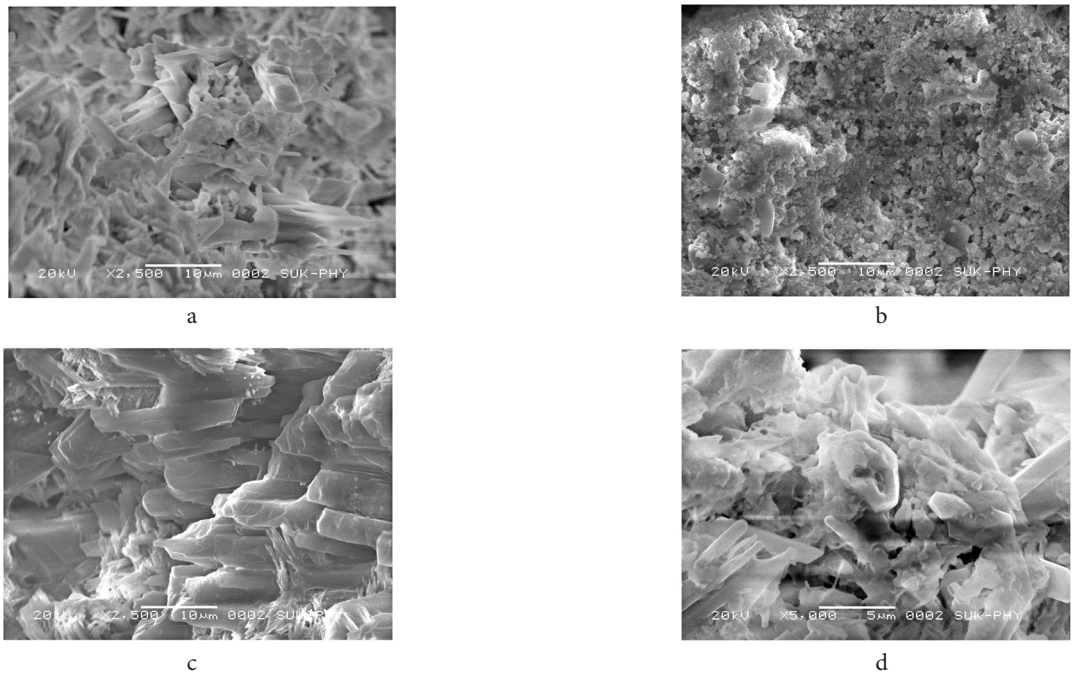

a b c d

Fig. 2. SEM images of the typical pure WO_3 nanostructures (a); SEM images 5 wt.% (b), 8 wt.% (c) and 15 wt.% (d) filler Cr-WO_3 nanomatrix.

introduction increases the absorbance of the nanoparticles from 300 to the 800 nm (visible region), the red shift in the spectrum is due to the increased addition of Cr to the WO_3 nanostructures facilitating the transfer of electrons to the WO_3 surface by capturing O_2^-, O^- ions by Cr_2O_3 formed on the nano matrix. The effect of surface polarization of Cr-WO_3 nano structures dominantly observed for heavily doped (15 wt.%) material with particle agglomeration. Fig. 3 clearly shows the addition of chromium leads to the displace of the edge of UV-spectrum (red shift) observed at 295 nm (UV-dip), 545 to 800 nm and possible attribution in red shift is due to the dissociation of chromium into the nano cavity of the WO_3.

4.4. XRD spectroscopy

XRD patterns of the pure WO_3 and Cr doped WO_3 NS (5, 8 and 15 wt.%) were recorded powder X-ray diffractometer with Cu-Kά (λ = 0.154 nm). Fig. 4 shows the XRD pattern of the pure WO_3 and different Cr doped WO_3. XRD pattern of change in tetrahedral geometry after the doping of the Cr into nano matrix of WO_3 was observed with the planes representing (002), (020), (200), (112), (022), (202), (222), (004) respectively. Intense peak Cr-WO_3 nanostructure was well matched with the JCPDS file no 75-2187 with (hkl) intensity values of Cr corresponds to (112), (022), (202), (004) respectively. The particle size was calculated by sheeres equation of the intense peak which was found to be 50 nm. Fig. 4 illustrates the X-ray diffraction patterns (XRD) of the Cr doped WO_3 nanostructures with crystal phase 2θ at 22°, 23°, 24°, 26°, 29°, 33, 44°, 50°, 54°, 56°, and 57° respectively. The crystallinity and the tetragonal crystal structure transforming to rod like structure of the 15 wt.% doped Cr was confirmed from the XRD measurements with the matching 2θ values of the crystal phase of pure WO_3.

4.5. I-V (current-voltage) characterization and impedance measurements

The *I-V* characteristics used to determine the total mobile charge carrier, leakage currents (*I*), resistance (*R*), voltage (*V*), conductance, admittance, impedance (*Z*), power dissipation (*P*) and time dependent conductivity performance of the sample as illustrated in Tables 2S and 3S (Supplementary Material) respectively. 15 wt.% of Cr doped WO_3 pelletized nanostructure was subjected for *I-V* measurements. Fig. 5 represents *I-V* curve of applied voltage vs. current and Fig. 2S (Supplementary Material) demonstrates impedance vs. bias voltage. The value of conductivity (1/*R*), admittance (1/impedance (*Z*)), impedance (*V*/*R*) and power dissipation (V^2/R) was calculated. The highest value of conductance, resistance, power dissipation, impedance for 15 wt.% of Cr doped WO_3 (Table 1) was found to be 5.664×10^{-5} S/m, 992478.1 Ώ, 2.52×10^{-5} W, 9.9 Ώ respectively. The highest power was 2.52×10^{-5} watts which indicate the Cr doped WO_3 nanostructure possess super-capacitor applications. The bias voltage varied between −6 to +6 V and the impedance of the pelletized Cr 15 wt.% doped WO_3 NS was investigated. The values of conductance, impedance, power dissipation for the 5 wt.% of Cr-WO_3 and 8 wt.% of Cr-WO_3 NS tabulated in Table 1.

5. Conclusion

In summary nano-crystalline materials of Cr doped WO_3 with different wt.% of Cr (5, 8 and 15 wt.%) synthesized by co precipitation method, characterized by CV, XRD,

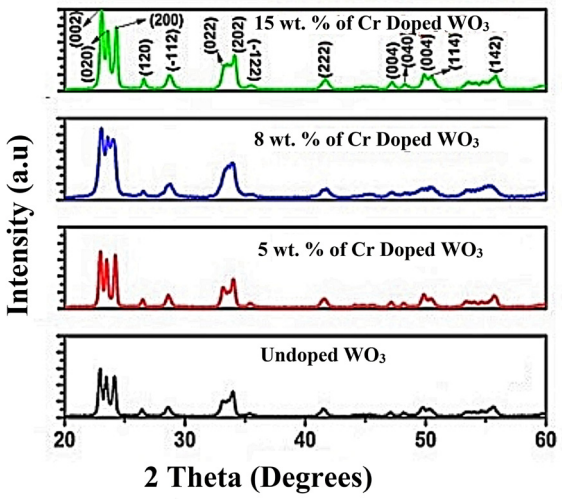

Fig. 4. (Color online) XRD-patterns of the pure WO_3 and 5, 8 and 15 wt.% of Cr nanostructures.

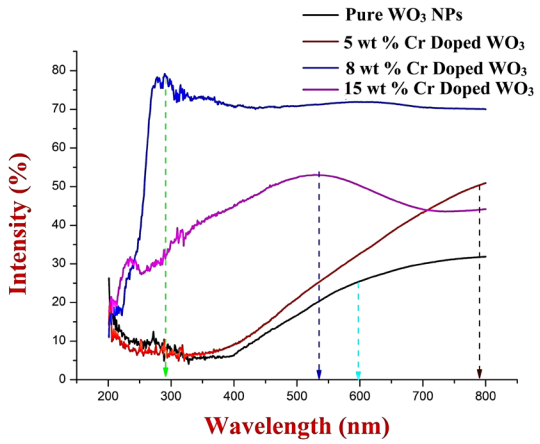

Fig. 3. (Color online) UV-visible overlay spectrum of the pure WO_3 and 5, 8, 15 wt.% of the Cr-WO_3 nanostructures.

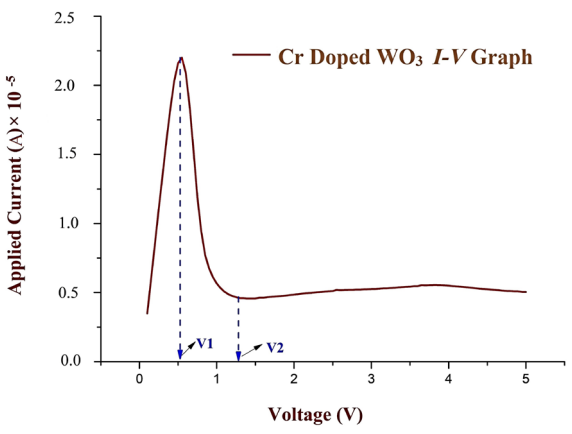

Fig. 5. The *I-V* graph of the pelletized Cr (15 wt.%) doped WO_3 nanostructures.

Table 1. Representing values of bias voltage, impedance and admittance for the 5, 8 and 15 wt.% of Cr-WO_3 nanostructures.

	Bias Voltage [V]	Impedance [Ω] × 10^5	Admittance [S/m] ×10^{-5}
Pelletized 5 wt.% Cr-WO_3	0.35	0.28	3.57
	0.75	0.68	1.47
	1.25	2.92	0.342
	5	12.5	0.08
Pelletized 8 wt.% Cr-WO_3	0.34	0.251	2.94
	0.75	0.630	1.33
	1.35	2.89	0.740
	5	9.9	0.101
Pelletized 15 wt.% Cr-WO_3	0.3	0.22	4.54
	0.75	0.630	1.58
	1.25	2.67	0.374
	5	9.9*	0.101

*Highest impedance

SEM, UV-Visible and studied for *I-V* and impedance measurements. XRD patterns reveal agglomerated tetragonal crystal structure transformed into rod like structures compared and agrees with the JCPDS file with intense peak planes matching with 2θ values for pure WO_3 and Cr-WO_3 nano particles. Average grain size for 15 wt.% of Cr-WO_3 was ~60 nm and grain boundary was ~90 nm. CV spectra indicate the band gap of the highest 15 wt.% doped material is 1.46 eV. UV absorption spectrum showed the absorption maxima at 800 nm for the 15 wt.% of Cr doped WO_3 nanostructures. *I-V*, impedance was recorded especially for 15 wt.% showed nonlinear relationship with the applied current, and considerably increase in the power output, admittance and surface conductivity was observed for the pelletized samples. The value of conductance, resistance, power dissipation, impedance for 15 wt.% of Cr doped WO_3 was found to be 5.664×10^{-5} S/m, 992478.1 Ω, 2.52×10^{-5} W, 9.9 Ω respectively. Increased power dissipation of 2.52×10^{-5} W facilitates 15 wt.% of Cr doped WO_3 nanostructure finds applications in super capacitor, biosensor, photodiodes etc.

Acknowledgements. All the authors are thankful to Ramaiah Institute of Technology, Bangalore, India, CENSE, IISc, Bangalore, Karnataka, India, Shivaji University, Kolhapur, Karnataka, India for their needful support for characterization and carrying out the necessary experimentations.

Supplementary Material. *The online version of this paper contains supplementary material (Figures and Tables) available free of charge at the journal's Web site (lettersonmaterials.com).*

References

1. F. Zhang. Frontiers in Chemistry. 5, 80 (2017). Crossref
2. M.S. Diallo, N.A. Fromer, M.S. Jhon. Journal of Nanoparticle Research. 15, 2044 (2013). Crossref
3. J. Jeevanandam, A. Barhoum, Y.S. Chan, A. Dufresne, M.K. Danquah. Beilstein Journal of Nanotechnology. 9, 1050 (2018). Crossref
4. E. Toto, M. Palombi, S. Laurenzi, M.G. Santonicola. Ceramics International. 45 (7), 9631 (2019). Crossref
5. K. Kang, Y. Cho, K.J. Yu. Micromachines. 9 (6), 263 (2018). Crossref
6. H. Zhu, Q. Li. Electronics. 8 (5), 564 (2019). Crossref
7. S.A. Moshizi, S. Azadi, A. Belford et al. Nano-Micro Letters. 12, 109 (2020). Crossref
8. I. Khan, K. Saeed, I. Khan. Arabian Journal of Chemistry. 12 (7), 908 (2019). Crossref
9. X.-F. Zhang, Z.-G. Liu, W. Shen, S. Gurunathan. International Journal of Molecular Sciences. 17, 1534 (2016). Crossref
10. J. Huang, J. Zeng, K. Zhu, R. Zhang, J. Liu. Nano-Micro Letters. 12, 110 (2020). Crossref
11. R. Liu. Materials. 7(4), 2747 (2014). Crossref
12. T.W. Kim, Y. Yang, F. Li, W.L. Kwan. NPG Asia Materials. 4, e18 (2012). Crossref
13. B.P. Nguyen, T. Kim, C.R. Park. Journal of Nanomaterials. 2014, 243041 (2014). Crossref
14. I.Y. Habib, A.A. Tajuddin, H.A. Noor et al. Scientific Reports. 9, 9207 (2019). Crossref
15. O. Sakhno, P. Yezhov, V. Hryn, V. Rudenko, T. Smirnova. Polymer. 12, 480 (2020). Crossref
16. W.E. Mahmoud. Journal of Physics D Applied Physics. 42, 155502 (2009). Crossref
17. J.H. Park, Y.T. Lim, O O. Park, J.K. Kim, J.-W. Yu, Y.C. Kim. Chemistry of Materials. 16 (4), 688 (2004). Crossref
18. T.-D. Nguyen. Nanoscale. 5, 9455 (2013). Crossref
19. F.L. Theiss, G.A. Ayoko, R.L. Frost. Applied Surface Science. 383, 200 (2016). Crossref
20. R. Herizchi, E. Abbasi, M. Milani, A. Akbarzadeh. Nano Medicine and Biotechnology. 44, 596 (2016). Crossref
21. Y. Wang, B. Liu, S. Xiao, X. Wang, L. Sun, H. Li, W. Xie, Q. Li, Q. Zhang, T. Wang. Applied Material International. 8 (15), 9674 (2016). Crossref
22. S.S. Kalanur. Catalysts. 9, 456 (2019). Crossref
23. J. Zhang, S.J. Deng, S.Y. Liu, J.M. Chen, B.Q. Han, Y. Wang, Y.D. Wang. Materials Technology. 29 (5), 262 (2014). Crossref
24. S.B. Upadhyay, R.K. Mishra, P.P. Sahay. Ceramics International. 42 (14), 15301 (2016). Crossref
25. W. Zhang, Y. Fan, T. Yuan, B. Lu, Y. Liu, Z. Li, G. Li, Z. Cheng, J. Xu. ACS Applied Materials & Interfaces. 12 (3), 3755 (2020). Crossref
26. K.L. Kelly, E. Coronado, L.L. Zhao, G.C. Schatz. Journal of Physical Chemistry B. 107 (3), 668 (2003). Crossref
27. D. Meng, N.M. Shaalan, T. Yamazaki, T. Kikuta. Sensors and Actuators B Chemical. 169, 113 (2012). Crossref
28. M. Parthibavarman, M. Karthik, P. Sathishkumar, R. Poonguzhali. Journal of the Iranian Chemical Society. 15, 1419 (2018). Crossref
29. P.A. Shinde, S.C. Jun. Chem Sus Chem. 13 (1), 11 (2020). Crossref
30. W. Li, P. Da, Y. Zhang, Y. Wang, X. Lin, X. Gong, G. Zheng. ACS Nano. 8 (11), 11770 (2014). Crossref
31. Z. Zhu, L. Zheng, S. Zheng, J. Chen, M. Liang, Y. Tian, D. Yang. Journal of Material Chemistry A. 6, 21419 (2018). Crossref